GEOPHYSICAL RESEARCH LETTERS, VOL. 35, L15201, doi:10.1029/2008GL034956, 2008

Fast and accurate estimation of solar irradiance on Martian slopes

Aymeric Spiga[1] and François Forget[1]

Received 7 June 2008; accepted 16 July 2008; published 15 August 2008.

[1] A general parameterization is proposed in this study to calculate, in a Mars-like dusty atmosphere, the solar irradiance reaching an inclined surface, assuming the value in the horizontal case is known. Complete Monte-Carlo radiative transfer calculations, using the Ockert-Bell et al. (1997) dust optical properties, enable the validation of the method for Mars. The total shortwave flux reaching the surface is composed of three contributions: direct incoming flux, reflected flux by surrounding terrains, and scattered flux by the atmospheric dust. The main difficulty is the parameterization of the latter component. We show that the scattered flux reaching the slope can be expressed by a physically-based simple formula involving one empirical coupling matrix and two vectors accounting for the scattering properties and the geometrical settings. The final result is a computationally efficient parameterization, with an accuracy in most cases better than 5 W.m^{-2}. Such a fast and accurate method to calculate solar irradiance on Martian slopes (should they be topographical surfaces or solar panels) is of particular interest in a wide range of applications, such as remote-sensing measurements, geological and meteorological models, and Mars exploration missions design. **Citation:** Spiga, A., and F. Forget (2008), Fast and accurate estimation of solar irradiance on Martian slopes, *Geophys. Res. Lett.*, *35*, L15201, doi:10.1029/2008GL034956.

1. Introduction

[2] An accurate knowledge of the illumination conditions on the Martian surface is a necessary prerequisite for space exploration studies, remote-sensing retrievals, energy balance models, and meteorological simulations. Steep topographical gradients are very common on Mars, two of the most dramatic examples being the Olympus Mons volcano and the Valles Marineris canyon. Thus, realistic representation of the solar irradiance on the Martian surface ought to take into account the inclination and the orientation of the topographical slope at the considered locations [*Schorghofer and Edgett*, 2006; *Aharonson and Schorghofer*, 2006; *Rafkin et al.*, 2002].

[3] This issue is especially crucial as recent remote-sensing measurements and imaging by Mars Express and Mars Reconnaissance Orbiter led the Martian geologists and atmospheric scientists to focus on the understanding of very local processes.

[4] Accurate calculations of irradiance on Martian slopes can be achieved by complete radiative transfer integrations. This possibility is however ruled out in many practical cases for computational cost reasons, and the complete integrations are usually replaced by crude irradiance estimations. Designing an accurate and computationally efficient parameterization of the insolation on Martian slopes is thus of particular interest. Description and validation of such a model are proposed in this paper. The practical problem is the following: given the sun position, the atmosphere opacity, and the value of radiative fluxes on an horizontal surface (calculated from radiative transfer code), how can the solar irradiance on a slope of given inclination and orientation be parameterized?

2. Definitions

2.1. Geometry

[5] Derived from the considered areocentric longitude L_s, local time and latitude, the cosine μ_0 of the solar zenith angle describes the position of the sun with respect to the local vertical. The horizontal orientation is given by the solar azimuth ψ_0.

[6] Similarly, a slope on Mars can be described by its inclination θ and orientation ψ. Let us consider a two-dimensional topographical field $h(x, y)$, for instance extracted from Mars Orbiter Laser Altimeter (MOLA) measurements. x and y are the distance in meters respectively in the longitude and the latitude direction. The slope inclination θ and the slope orientation ψ may be straightforwardly computed from $\tan\theta = \sqrt{h_x^2 + h_y^2}$ and $\tan\psi = h_y/h_x$, where the topographical function derivatives are $h_x = \partial h/\partial x$ and $h_y = \partial h/\partial y$. In what follows, θ is chosen as positive, which means any sign consideration is transferred to the azimuth angle ψ (assumed to be oriented with the same convention as ψ_0).

[7] A critical quantity in the slope insolation problem is the cosine μ_s of the angle between the incident sun rays and the normal to the slope. μ_s can be calculated from θ, μ_0 (which of course must be >0), ψ and ψ_0:

$$\mu_s = \max\left[0\,,\ \mu_0\,\cos\theta + \sqrt{1-\mu_0^2}\,\sin\theta\,\cos\left(\psi-\psi_0\right)\right] \qquad (1)$$

Another crucial geometrical quantity is the sky-view factor:

$$\sigma_s = \frac{1+\cos\theta}{2} \qquad (2)$$

which quantifies the proportion of the sky in the half hemisphere "seen" by the slope that is not obstructed by the surrounding terrain (assumed to be flat). Complementarily, the terrain-view factor can be defined as $\sigma_t = 1 - \sigma_s$: the more tilted the surface is, the more exposed to the reflected

[1]Laboratoire de Météorologie Dynamique, UPMC BP99, Institut Pierre-Simon Laplace, Université Pierre et Marie Curie, Centre National de la Recherche Scientifique, Paris, France.

0094-8276/08/2008GL034956$05.00

radiation by the surrounding terrains it is. We adopt in the present study the simple trigonometric formula for σ_t and σ_s by *Kondratyev* [1965], but more sophisticated calculations might be found in work by *Dozier and Frew* [1990].

2.2. Monte-Carlo Reference Code

[8] In order to build and validate the parameterization, a reference Monte-Carlo radiative transfer code is used in this study. The Monte-Carlo tool calculates, in plane-parallel geometry, the sun illumination on any point of the Mars surface at anytime and for any slope orientation [*Tran and Rannou*, 2004]. At each spectral band, the Monte-Carlo simulation keeps track of three-dimensional trajectories of photons, which randomly walk inside the atmosphere from the top of the atmosphere in the initial solar direction, until the photons disappear by absorption or escaping the atmosphere. The model records the complete angular distribution of photons reaching the surface, and thus the exact flux reaching a flat panel at the Mars surface (i.e. the total solar irradiance in W.m^{-2}) oriented in any direction. Absorption and scattering of solar light by dust aerosols are calculated with dust radiative properties derived from the work by *Ockert-Bell et al.* [1997] (spectrally-averaged single-scattering albedo and asymmetry parameter [ω, g] are [0.665, 0.819] in the range 0.1–0.5 μm and [0.927, 0.648] in the range 0.5–5 μm). Accuracy of the model is of order 1% when the number of photons per spectral band reaches 10^5, which was the choice for the present study.

3. Direct and Reflected Irradiance on Slopes

[9] The total solar irradiance $\mathcal{F}$ on a given unit surface with slope angles (θ, ψ) can be split in three distinct parts: direct incoming flux from the sun $\mathcal{D}$, scattered flux by dust in the Martian atmosphere $\mathcal{S}$, reflected flux from the neighboring terrains $\mathcal{R}$. Hereinafter, we assume that the fluxes $\mathcal{F}_0$, $\mathcal{D}_0$ and $\mathcal{S}_0$ on a Martian horizontal surface are known. These fluxes can be calculated for instance by two-stream fast radiative transfer models [*Savijärvi et al.*, 2005; *Forget et al.*, 1999].

[10] The direct component $\mathcal{D}$ can merely be derived from considerations of projection, as μ_s may be regarded as the normalized insolation on the slope:

$$\mathcal{D} = \frac{\mu_s}{\mu_0}\,\mathcal{D}_0 \tag{3}$$

[11] The reflected component $\mathcal{R}$ can be calculated under the assumption of Lambertian surface with albedo A_L:

$$\mathcal{R} = (1-\sigma_s)\,A_L\,(\mathcal{D}_0 + \mathcal{S}_0) \tag{4}$$

[12] Comparisons of the above formula calculations with results from Monte-Carlo computations, where the photon-by-photon strategy allows for distinct estimation of the three irradiance components, show excellent agreement ($\ll$1 W.m^{-2}). Directional effects on non-Lambertian surfaces for the reflected sunlight may yield slightly different results for $\mathcal{R}$. However, since the values observed for $\mathcal{R}$ are low compared to the two other components $\mathcal{D}$ and $\mathcal{S}$, the reflection directional effects were not considered in this study.

4. Scattered Irradiance on Slopes

[13] The most difficult part of the problem is to find an accurate representation of the scattered component $\mathcal{S}$ of the total solar irradiance reaching the tilted surface. The parameterization of this flux may be formulated as the search for a function f of the main parameters such as $\mathcal{S} = \mathcal{S}_0\,f(\mu_0, \mu_s, \theta, \tau)$, where τ is the visible dust column optical depth at the reference wavelength 0.67 μm.

[14] The contribution of $\mathcal{S}$ on the total flux $\mathcal{F}$ is of particular significance in the case of the dusty Martian atmosphere. When τ is above 0.7, the scattered solar flux can even exceed the direct component at the surface [*Savijärvi et al.*, 2005].

[15] An example is given in Table 1, with typical parameters describing the landing site environment of the Spirit rover: latitude is 15°S, L_s is 330°, dust opacity is τ = 0.3 (measured by the mini-TES instrument [*Smith et al.*, 2006] and converted with τ_{vis}/τ_{ir} = 2), and albedo is 0.2. Even if the Martian atmosphere is moderately dusty, in the morning and in the end of the afternoon, the ratio $\mathcal{S}_0/\mathcal{D}_0$ reaches 1/2 (and 1/4 at noon). Moreover, east-facing slope calculations confirm that $\mathcal{S}$ and $\mathcal{D}$ variations due to surface tilting are significant.

4.1. Background

[16] Similar studies have been conducted for the terrestrial atmosphere [*Muneer*, 2004], often motivated by solar energy issues [*Capderou*, 1988], remote-sensing measurements in mountainous regions [*Sandmeier and Itten*, 1997], or mesoscale modeling [*Müller and Scherer*, 2005; *Senkova et al.*, 2007].

[17] *Hay and Davies* [1978] proposed a linear ponderation between an anisotropic component, which predominates in the case of clear-sky conditions, and an isotropic component, which predominates in the case of overcast skies:

$$\frac{\mathcal{S}}{\mathcal{S}_0} = \kappa\,\frac{\mu_s}{\mu_0} + (1-\kappa)\,\sigma_s$$

where $0 < \kappa < 1$ is the anisotropy factor, depending on the atmospheric transmittance $e^{-\tau}$. The anisotropic contribution (first term of the addition) is assumed to be predominantly caused by the forward scattered flux enhancement in the circumsolar region of the sky; its expression is thus directly inspired from equation (3) for the direct flux $\mathcal{D}$.

[18] The simplified assumptions of the Hay model did not prevent it to be rather accurate in a wide range of realistic applications [*Bird and Riordan*, 1986]. A model very similar to the Hay approach was employed to assess the formation of Martian gullies [*Costard et al.*, 2002, footnote 24], and led to satisfying diagnostics. Tests were carried out to adapt in the Martian environment the Hay model to a wider range of sun position and slope geometry. Unfortunately, attempts to derive the κ parameter from computed Monte-Carlo values $\mathcal{S}$ were often unsuccessful: unrealistic and/or θ-dependent values were found, resulting from the inability

Table 1. Solar Irradiance Reaching a Surface Located at the Spirit Landing Site[a]

		Irradiance (W.m^{-2})			
Local Time	θ (°)	$\mathcal{F}$	$\mathcal{S}$	$\mathcal{D}$	$\mathcal{R}$
08AM	0	283	97	186	0
	15	387	129	257	1
12AM	0	592	130	462	0
	15	575	127	446	2
04PM	0	282	96	186	0
	15	170	66	103	1

[a]Shown are horizontal terrain and east-facing 15° slope. Visible dust opacity is $\tau = 0.3$.

of the model to correctly represent the relative contribution from the anisotropic and the isotropic components.

[19] *Perez et al.* [1990] refined the Hay model with the inclusion of the "horizon brightening" anisotropic component (due to enhanced aerosol scattering in the direction of the horizon) and the introduction of more flexibility into the linear coefficients:

$$\frac{\mathcal{S}}{\mathcal{S}_0} = \kappa_1 \frac{\mu_s}{\mu_0} + (1-\kappa_1)\,\sigma_s + \kappa_2 \sin\theta$$

In the three-component Perez model, κ_1 and κ_2 are linear functions of atmospheric transmittance and solar zenith angle, with sets of linear coefficients empirically defined for different categories of sky brightness. The Perez refinements were shown to improve the slope flux calculations on Earth, compared to the Hay model [*Li and Lam*, 2000]. In the Martian case, derivation of the Perez linear coefficients κ_1 and κ_2 in a few examples improved the parameterized estimations of $\mathcal{S}$ too. Some problems however remained. On the one hand, the balance between isotropic and anisotropic contribution was not satisfyingly accounted for. On the other hand, our somewhat heuristic approach for calculations of the Perez coefficients was difficult to generalize.

4.2. Martian Model

[20] Discussion in the previous subsection shows that, compared to the Perez model, the Martian model has to allow for more degrees of freedom in the parameterization. In other words, the general principle of additive splitting between horizon anisotropic, circumsolar anisotropic, and isotropic components is kept, as well as the use of linear functions, but the starting point of the Martian parameterization is a generalized formula:

$$\frac{\mathcal{S}}{\mathcal{S}_0} = \mathcal{K}_1(\mu_0, e^{-\tau}, \sin\theta)\,\frac{\mu_s}{\mu_0} + \mathcal{K}_2(\mu_0, e^{-\tau})\,\sigma_s + \mathcal{K}_3(\mu_0, e^{-\tau}, \sin\theta)$$

[21] Systematic Monte-Carlo calculations were carried out for different μ_0, $e^{-\tau}$, θ, ψ parameters to assess the behavior of $\mathcal{K}_1$, $\mathcal{K}_2$, and $\mathcal{K}_3$:

[22] 1. Slope inclinations θ ranged from 0° to 45°, with 2° resolution.

[23] 2. All slope orientations ψ were considered, with 15° resolution.

[24] 3. Dust opacity τ ranged from 0.1 to 1, with 0.1 resolution; calculations were also performed in the dustier cases τ = 1.5, 2, 2.5, 3, 3.5, 4, 6, 9.

[25] 4. Cosine of solar zenith angle μ_0 ranged from 0.15 to 1.

[26] The linear behavior of $\mathcal{S}/\mathcal{S}_0$ with μ_s/μ_0 was excellent for any given (μ_0, $e^{-\tau}$, θ) triplet. Linear correlation coefficients were also satisfying when assessing, for a given sun position μ_0, the variations of $\mathcal{K}_1$ and $\mathcal{K}_3$ with $e^{-\tau}$ and sinθ, and $\mathcal{K}_2$ with $e^{-\tau}$. Departures from linearity were however identified out of the $0 < \theta < 30°$ and $0.1 < \tau < 1$ intervals. Finally, on the condition that we separately consider positions of the sun high in the sky ($\mu_0 \geqslant 0.5$) and low in the sky ($\mu_0 < 0.5$), linear coefficients of the $\mathcal{K}_i$ functions were themselves approximatively linearly varying with μ_0.

5. Parameterization of Scattered Irradiance on Martian Slopes

5.1. Description

[27] Given the successful step-by-step linear tests carried out in the previous section, the Martian generalized parametrization for the scattered irradiance on a slope can be written using a simple matrix formulation:

$$\mathcal{S} = \mathcal{S}_0\,\mathbf{s}^{\mathrm{t}} \times (\mathbf{M} + \mu_0\,\mathbf{N}) \times \mathbf{g} \tag{5}$$

where

[28] 1. **s** is a "scattering" vector (slope versus sky), both accounting for the isotropic scattered component and the anisotropic horizon brightening component:

$$\mathbf{s} = \begin{bmatrix} 1 \\ e^{-\tau} \\ \sin\theta \\ e^{-\tau}\sin\theta \end{bmatrix} \tag{6}$$

[29] 2. **g** is a "geometry" vector (slope versus sun), with first component accounting for the circumsolar contribution:

$$\mathbf{g} = \begin{bmatrix} \mu_s/\mu_0 \\ 1 \end{bmatrix} \tag{7}$$

[30] 3. **M** and **N** are two numerical 4 × 2 coupling matrices, empirically determined from the Monte-Carlo reference calculations during the step-by-step linear tests. For $\mu_0 \geqslant 0.5$, the coupling matrices are:

$$\mathbf{M} = \begin{bmatrix} -0.264 & 1.291\,\sigma_s \\ 1.309 & -1.371\,\sigma_s \\ 0.208 & -0.581 \\ -0.828 & 1.641 \end{bmatrix} \quad \mathbf{N} = \begin{bmatrix} 0.911 & -0.933\,\sigma_s \\ -0.777 & 0.822\,\sigma_s \\ -0.223 & 0.514 \\ 0.623 & -1.195 \end{bmatrix} \tag{8}$$

(with the 10^{-3} accuracy being necessary for the $\mu_0 \sim 1$ calculations), and for $\mu_0 < 0.5$ the coupling matrices are:

$$\mathbf{M} = \begin{bmatrix} -0.373 & 1.389\,\sigma_s \\ 0.792 & -0.794\,\sigma_s \\ -0.095 & -0.325 \\ 0.398 & 0.183 \end{bmatrix} \quad \mathbf{N} = \begin{bmatrix} 1.079 & -1.076\,\sigma_s \\ 0.275 & -0.357\,\sigma_s \\ 0.419 & -0.075 \\ -1.855 & 1.844 \end{bmatrix} \tag{9}$$

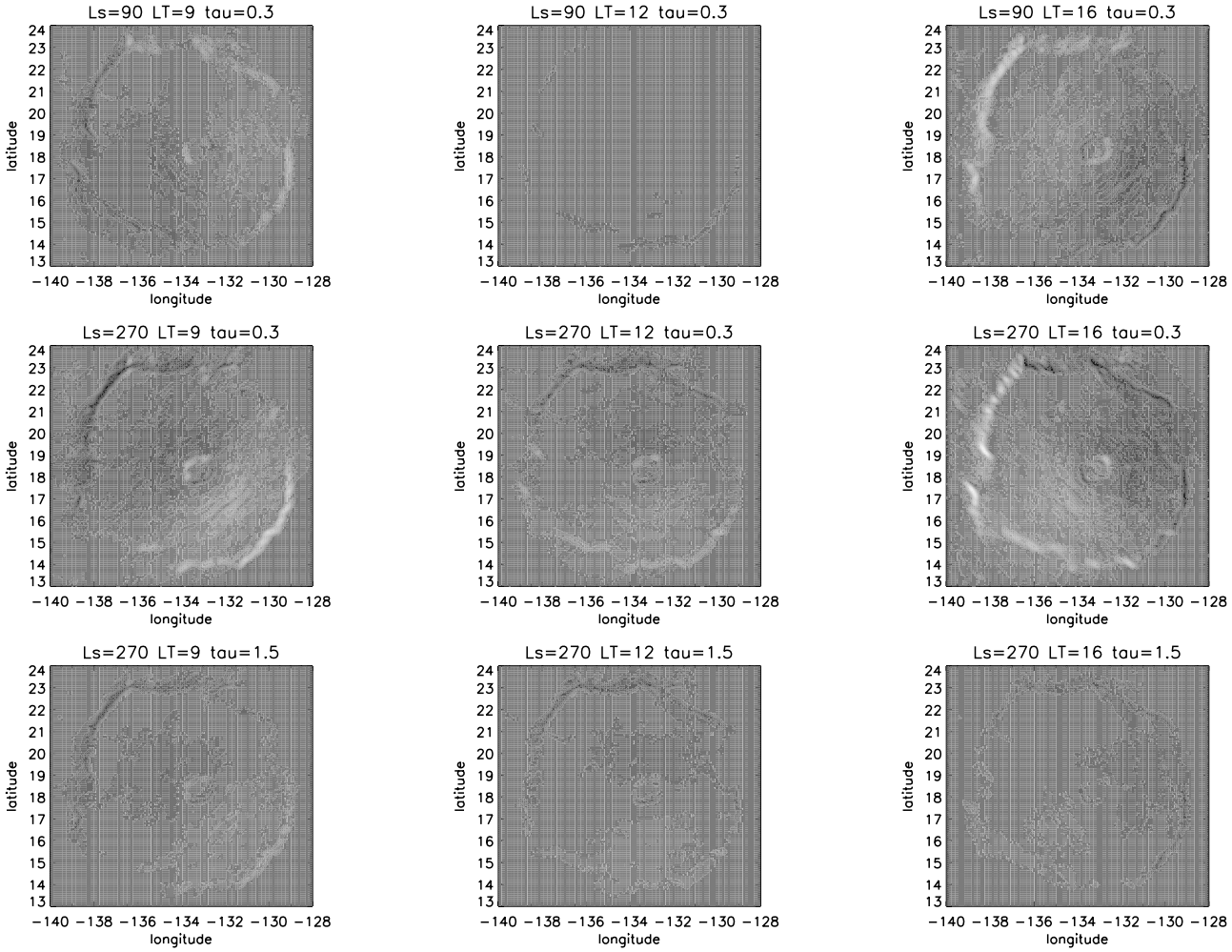

Figure 1. Parameterized ratio $\mathcal{S}/\mathcal{S}_0$ (%) (black is 30% and white is 170%) for the Olympus Mons region at northern summer solstice, northern winter solstice and dusty northern winter solstice. Topography and slope angles were calculated from the MOLA topographical data interpolated on a 5 km resolution grid. Maximum slope inclination θ is 27°. Each map (~22,500 points) was computed on a PC within 1 second using an IDL version of the parameterization.

Interestingly, none of the coupling matrices coefficients is negligible compared to the others, which may be regarded as an *a posteriori* validation of the adopted generalized approach.

[31] It must be emphasized that this linear formula, involving only one matrix/vector product and one dot product, is computationally very efficient. In addition, its implementation is straightforward whatever the programming language may be. An example of application in the Olympus Mons region is shown in Figure 1.

[32] For any μ_0 and τ, $\mathcal{S}/\mathcal{S}_0$ is obviously equal to 1 when the slope inclination $\theta = 0$. This leads to 4 constraints on the matrix coefficients: $m_{11} + m_{12} = 1$, $m_{21} + m_{22} = 0$, $n_{11} + n_{12} = 0$, $n_{21} + n_{22} = 0$. A glance at the coupling matrices shows the agreement with those constraints is imperfect. One consequence is that $\mathcal{S}/\mathcal{S}_0$ is not exactly equal to 1, but the resulting error at low angles ($\theta \leqslant 5°$) is negligible (<1 W.m^{-2}), whereas constraining the matrices coefficients would lead to significant errors at higher angles.

5.2. Performance

[33] Performance of the parameterization is very good for a wide range of insolation conditions, dusty atmosphere, slope orientation and inclination. As mentioned in the previous subsection, satisfactory linear behavior is observed in the Monte-Carlo reference values for $\theta \leqslant 30°$, $\tau \leqslant 1$, and $\mu_0 \geqslant 0.5$. However, linear assumptions also yield correct results (if not perfect) for the extended cases $\theta \leqslant 40°$, $\tau \leqslant 9$, and $\mu_0 \geqslant 0.15$.

[34] An illustrative example of the typical maximal differences between the parameterized scattered irradiance $\mathcal{S}$ and their reference Monte-Carlo counterparts is summarized in Table 2. In most cases, the maximal error on the scattered irradiance is below 5 W.m^{-2}, and the relative error is below 7% (note that the error on the total flux is lower).

[35] The performances are slightly degraded for inclinations $30° < \theta \leqslant 40°$ but remains rather acceptable (tests carried out with $1 < \tau \leqslant 9$ showed a similar performance degradation, which was not pronounced enough to completely rule out the parameterization, except for very low values of μ_s/μ_0). In case of clear Martian atmosphere and steep slope not facing the sun, or sun rather low in the sky, the maximal error can be of higher amplitude, and might even reach 15 W.m^{-2} (with a corresponding relative error of 15%) or 33% (with a corresponding absolute error of 9 W.m^{-2}).

Table 2. Error Maximal Absolute and Relative Errors of Parameterized Scattered Component of the Total Solar Irradiance[a]

		With Parameterization				Without Parameterization			
		$\delta\mathcal{S}_{max}$[b] (W.m^{-2})		$(\delta\mathcal{S}/\mathcal{S})_{max}$[b] (%)		$\delta\mathcal{S}_{max}$[b] (W.m^{-2})		$(\delta\mathcal{S}/\mathcal{S})_{max}$[b] (%)	
Sun Position	Orientation[c]	Min[d]	Max[d]	Min[d]	Max[d]	Min[d]	Max[d]	Min[d]	Max[c]
$\mu_0 = 0.83$	NE	2 (3)	8 (14)	3 (9)	7 (14)	13 (16)	60 (81)	50 (80)	47 (73)
($L_s = 90°$)	SE	0 (1)	5 (9)	0 (1)	3 (5)	8 (12)	25 (39)	13 (22)	14 (25)
	SW	1 (2)	4 (6)	0 (1)	2 (4)	23 (25)	27 (27)	17 (18)	23 (26)
	NW	0 (1)	4 (8)	0 (1)	2 (4)	1 (3)	11 (22)	2 (7)	6 (12)
$\mu_0 = 0.56$	NE	5 (6)	13 (17)	13 (19)	24 (34)	24 (27)	70 (87)	75 (113)	115 (162)
($L_s = 180°$)	SE	0 (0)	4 (6)	1 (1)	3 (4)	3 (3)	5 (13)	2 (4)	3 (9)
	SW	1 (4)	5 (8)	1 (2)	4 (7)	55 (66)	51 (57)	33 (36)	41 (46)
	NW	0 (0)	5 (8)	0 (1)	4 (6)	4 (8)	23 (35)	16 (26)	16 (26)
$\mu_0 = 0.18$	NE	4 (4)	6 (8)	18 (24)	29 (45)	19 (21)	28 (32)	58 (82)	157 (199)
($L_s = 270°$)	SE	0 (1)	4 (5)	1 (1)	7 (8)	3 (3)	12 (14)	6 (6)	19 (21)
	SW	0 (1)	15 (19)	0 (1)	15 (19)	14 (16)	44 (54)	24 (26)	47 (52)
	NW	3 (3)	9 (9)	8 (8)	33 (35)	7 (11)	13 (15)	23 (35)	42 (53)

[a]References are Monte-Carlo radiative transfer calculations. Latitude is 50°N and local time is 02PM. Error values if no parameterization is applied (i.e. assuming that $\mathcal{S} = \mathcal{S}_0$ whatever the slope inclination and orientation may be) are also reported to give clues on the usefulness and the accuracy of the proposed parameterization.

[b]$\delta\mathcal{S}_{max}$ denotes the maximal values of the absolute error on the scattered flux $\mathcal{S}$, calculated for θ ranging from 0 to 30° (40° for bracketed numbers). The same terminology applies to the relative error $(\delta\mathcal{S}/\mathcal{S})_{max}$ on the scattered flux $\mathcal{S}$.

[c]The orientations chosen in this table are those for which the error values are the highest.

[d]Maximum and minimum values of $\delta\mathcal{S}_{max}$ and $(\delta\mathcal{S}/\mathcal{S})_{max}$ are calculated for τ ranging from 0.1 to 1.

[36] Out of these extreme situations, pointing out the limits of the linear approach adopted in this paper, the parameterization performances are excellent: the vast majority of comparisons between parameterized and reference fluxes show differences below 3 W.m^{-2}. For instance, errors on the parameterized scattered irradiances in the Spirit example, with a 15° east-facing slope, are less than 1.5 W.m^{-2} at the three considered local times. Furthermore, an extension of the analysis presented in Table 2 to a wider range of parameters shows that the root mean square error (respectively the mean absolute error) of the linear parameterization for scattered flux with respect to the Monte-Carlo reference is 2.2 (1.4) W.m^{-2} for $\theta \leqslant 30°$ and $\tau \leqslant 1$; 2.7 (1.6) W.m^{-2} if $\theta \leqslant 40°$; and 3.6 (2.2) W.m^{-2} if $\tau \leqslant 4$.

6. Conclusion

[37] The purpose of the study was to find a simple method to calculate the total solar irradiance on Martian slopes, with minimum knowledge of the geometry and the fluxes reaching an horizontal surface, as computed by all Mars atmosphere models. The semi-empirical approach proposed in this paper, based on physical considerations, is an accurate and computationally efficient answer to the problem. It was validated in the whole range of realistic Martian illumination conditions and topographical slopes. The outline of this Martian parameterization, which will be a useful tool for numerous applications, from remote-sensing retrieval codes to geological and meteorological models, is the following:

[38] 1. deduce μ_0 and ψ_0 from L_s, local time and latitude.

[39] 2. compute μ_s with equation (1).

[40] 3. calculate σ_s with equation (2).

[41] 4. compute $\mathcal{D}$ with equation (3).

[42] 5. compute $\mathcal{R}$ with equation (4).

[43] 6. compute $\mathcal{S}$ with equation (5) using the ''scattering'' vector **s** (equation (6)), the ''geometry'' vector **g** (equation (7)), and the coupling matrices (equations (8) and (9)) empirically validated in the present paper.

[44] 7. deduce the total solar irradiance $\mathcal{F} = \mathcal{D} + \mathcal{R} + \mathcal{S}$

[45] We used in this study the reference *Ockert-Bell et al.* [1997] dust optical properties, cross-validated upon the *Tomasko et al.* [1999] measurements from the surface. Recent measurements from orbit by A. Määttänen et al. (A study of the properties of a local dust storm with Mars Express OMEGA and PFS data, submitted to Icarus, 2008) and M. J. Wolff and M. Vincendon (personal communication, 2008) have shown that the dust might be less absorbent than previously determined by *Ockert-Bell et al.* [1997]. To assess the effect of such a slight underestimation of the scattered flux incoming from the airborne dust, we compared the results of the parameterization with reference Monte-Carlo calculations using the *Clancy and Lee* [1991] brighter dust properties. The errors on the total flux were found to be below 6% in most cases, and for the most difficult situations (low μ_s, low μ_0, high τ), do not exceed the maximal errors mentioned in the paper. Future improvements of the present parameterization, consisting in slight modifications of the matrices coefficients to be in better agreement with the upcoming revised dust optical properties, will however be considered. Alternative formula for σ_s based on more realistic considerations, inclusion of directional effects in the $\mathcal{R}$ calculations, and solutions for better accuracy on terrains receiving less irradiance, will be investigated too as future improvements of the model.

[46] We might finally mention, to complete the description of the Martian radiative environment, that an accurate estimation of the thermal infrared incident flux $\mathcal{T}$ on the inclined surface is also required. To first order, one can assume that the atmospheric thermal radiation is isotropic. Similarly to the aforementioned use of the sky-view factor σ_s and the terrain-view factor σ_t, the following simple correction can thus be proposed:

$$\mathcal{T} = \sigma_s \mathcal{T}_0 + \sigma_t \mathcal{E}$$

where $\mathcal{T}_0$ is the atmospheric incident thermal IR flux on an horizontal surface and $\mathcal{E} = \epsilon\sigma T_s^4$ is the thermal emission (σ is the Stefan-Boltzmann constant) from the surrounding terrains with emissivity $\mathcal{E}$ and temperature T_s.

[47] **Acknowledgments.** We thank M. J. Wolff and M. Capderou for helpful discussion, T. T. Tran for the development of the Monte Carlo model and ESA (S. Zimmermann) for support in its development. The authors thank two anonymous reviewers for their constructive comments and suggestions.

References

Aharonson, O., and N. Schorghofer (2006), Subsurface ice on Mars with rough topography, *J. Geophys. Res.*, *111*, E11007, doi:10.1029/2005JE002636.

Bird, R. E., and C. Riordan (1986), Simple solar spectral model for direct and diffuse irradiance on horizontal and tilted planes at the Earth's surface for cloudless atmospheres, *J. Appl. Meteorol.*, *25*, 87–97.

Capderou, M. (1988), *Atlas Solaire de l'Algérie*, Off. des Publ. Univ., Alger.

Clancy, R. T., and S. W. Lee (1991), A new look at dust and clouds in the Mars atmosphere: Analysis of emission-phase function sequences from global Viking IRTM observations, *Icarus*, *93*, 135–158.

Costard, F., F. Forget, N. Mangold, and J. P. Peulvast (2002), Formation of recent Martian debris flows by melting of near-surface ground ie at high obliquity, *Science*, *295*, 110–113.

Dozier, J., and J. Frew (1990), Rapid calculation of terrain parameters for radiation modeling from digital elevation data, *IEEE Trans. Geosci. Remote Sens.*, *28*(5), 963–969.

Forget, F., F. Hourdin, R. Fournier, C. Hourdin, O. Talagrand, M. Collins, S. R. Lewis, P. L. Read, and J.-P. Huot (1999), Improved general circulation models of the Martian atmosphere from the surface to above 80 km, *J. Geophys. Res.*, *104*, 24,155–24,176.

Hay, J. E., and J. A. Davies (1978), Calculation of the solar radiation incident on an inclined surface, in *Proceedings of the First Canadian Solar Radiation Data Workshop*, edited by J. E. Hay and T. K. Won, pp. 59–72, Minist. of Suppl. and Serv., Toronto, Ont., Canada.

Kondratyev, K. Y. (1965), *Radiative Heat Exchange in the Atmosphere*, Pergamon, Oxford, U. K.

Li, D. H. W., and J. C. Lam (2000), Evaluation of slope irradiance and illuminance models against measured Hong Kong data, *Build. Environ.*, *35*(6), 501–509.

Müller, M. D., and D. Scherer (2005), A grid and subgrid scale radiation parameterization of topographic effects for mesoscale weather forecast models, *Mon. Weather Rev.*, *133*, 1431–1442.

Muneer, T. (2004), *Solar Radiation and Daylight Models*, Butterworth-Heinemann, Oxford, U. K.

Ockert-Bell, M. E., J. F. Bell III., C. McKay, J. Pollack, and F. Forget (1997), Absorption and scattering properties of the Martian dust in the solar wavelengths, *J. Geophys. Res.*, *102*, 9039–9050.

Perez, R., P. Ineichen, R. Seals, J. Michalsky, and R. Stewart (1990), Modelling daylight availability and irradiance components from direct and global irradiance, *Sol. Energy*, *44*, 271.

Rafkin, S. C. R., M. R. V. Sta. Maria, and T. I. Michaels (2002), Simulation of the atmospheric thermal circulation of a Martian volcano using a mesoscale numerical model, *Nature*, *419*, 697–699.

Sandmeier, S., and K. I. Itten (1997), A physically-based model to correct atmospheric and illumination effects in optical satellite data of rugged terrain, *IEEE Trans. Geosci. Remote Sens.*, *35*(3), 708–717, doi:10.1109/36.581991.

Savijärvi, H., D. Crisp, and A.-M. Harri (2005), Effects of CO_2 and dust on present-day solar radiation and climate on Mars, *Q. J. R. Meteorol. Soc.*, *131*, 2907–2922.

Schorghofer, N., and K. S. Edgett (2006), Seasonal surface frost at low latitudes on Mars, *Icarus*, *180*, 321–334, doi:10.1016/j.icarus.2005.08.022.

Senkova, A. V., L. Rontu, and H. Savijärvi (2007), Parametrization of orographic effects on surface radiation in HIRLAM, *Tellus, Ser. A*, *59*, 279–291, doi:10.1111/j.1600-0870.2007.00235.x.

Smith, M. D., M. J. Wolff, N. Spanovich, A. Ghosh, D. Banfield, P. R. Christensen, G. A. Landis, and S. W. Squyres (2006), One Martian year of atmospheric observations using MER Mini-TES, *J. Geophys. Res.*, *111*, E12S13, doi:10.1029/2006JE002770.

Tomasko, M. G., L. R. Doose, M. Lemmon, P. H. Smith, and E. Wegryn (1999), Properties of dust in the Martian atmosphere from the Imager on Mars Pathfinder, *J. Geophys. Res.*, *104*, 8987–9008, doi:10.1029/1998JE900016.

Tran, T. T., and P. Rannou (2004), Comparing 3D spherical Monte-Carlo and 2-stream parallel plane simulation of far-field backscattering image of Titan, *Notes du Pole 2*, Inst. Pierre Simon Laplace, Paris.

F. Forget and A. Spiga, Laboratoire de Météorologie Dynamique, UPMCBP99, Institut Pierre-Simon Laplace, Université Pierre et Marie Curie, CNRS, 4, place Jussieu, F-75252 Paris CEDEX 05, France. (forget@lmd.jussieu.fr; spiga@lmd.jussieu.fr)